

# Core Loss Reduction of an Interior Permanent-Magnet Synchronous Motor Using Amorphous Stator Core

Shotaro Okamoto, Nicolas Denis, *Member, IEEE*, Yoshiyuki Kato, Masaharu Ieki, and Keisuke Fujisaki, *Senior Member, IEEE*

**Abstract**—The core losses of an interior permanent-magnet synchronous motor (PMSM) have been reduced by about 50% using an amorphous magnetic material (AMM) stator core instead of a nonoriented (NO) steel stator core. Numerical calculation and experimental tests data have been compared to evaluate the reliability of the results. The AMM stator core has been realized using the latest improvements in manufacturing technologies.

**Index Terms**—Amorphous magnetic material, magnetic cores, magnetic losses, permanent-magnet motor.

## I. INTRODUCTION

THE THREE main types of losses in rotational electrical machines are the mechanical losses caused by the friction with air and between mechanical parts, the copper losses due to coils resistance, and the core losses caused by the variation of the magnetic flux in the core parts. Both the mechanical and copper losses have been extensively investigated but the core loss phenomenon is yet to be completely understood by the scientific and engineer communities. Research studies are still carried out to reduce, understand, and evaluate these losses.

Since amorphous magnetic material (AMM) has superior characteristics as high resistivity and low coercive force, it offers potential reduction of iron loss, especially at high frequency [1]. The AMM has successfully been used for transformers' applications. It was found that the no-load losses of transformers could be reduced by up to 70% when AMM was used instead of grain-oriented silicon iron [2]. However, due to its high magnetostriction, the AMM magnetic properties can deteriorate and its iron losses increase in case of external magnetic field application [1]. The heat treatment also has an important role in the magnetic properties of the amorphous material, like magnetic permeability and coercive force [3].

Manuscript received June 5, 2015; revised July 28, 2015 and September 27, 2015; accepted September 29, 2015. Date of publication February 18, 2016; date of current version May 18, 2016. Paper 2015-EMC-0292.R2, presented at the 2015 IEEE International Electric Machines and Drives Conference, Coeur d'Alene, ID, USA, May 10–13, and approved for publication in the IEEE TRANSACTIONS ON INDUSTRY APPLICATIONS by the Electric Machines Committee of the IEEE Industry Applications Society. This work was supported by KAKENHI under Grant 26420259 of Ministry of Education, Culture, Sports, Science and Technology, Japan.

The authors are with the Toyota Technological Institute, Nagoya 468-8511, Japan (e-mail: sd10008@toyota-ti.ac.jp; nicolas.denis@toyota-ti.ac.jp; sd11016@toyota-ti.ac.jp; sd11002@toyota-ti.ac.jp; fujisaki@toyota-ti.ac.jp).

Color versions of one or more of the figures in this paper are available online at <http://ieeexplore.ieee.org>.

Digital Object Identifier 10.1109/TIA.2016.2532279

Moreover, the AMM is also sensitive to mechanical stress and its iron losses can increase due to core manufacture [2], [4]. The AMM sheets are very thin and have high mechanical brittleness, which result in difficult magnetic core manufacturing. However, the technological advances in amorphous ribbons manufacturing have permitted improvements in surface quality, resulting in higher lamination factor [5]. In addition, new cutting techniques made the manufacture of electrical motor cores easier [6]–[8].

Therefore, several kinds of electrical motors using amorphous cores have been developed. Since the core losses increase with the motor speed, the AMM can bring substantial improvement over conventional electrical steel sheets for high-speed applications [9], [10]. Moreover, since the cost of magnets is relatively high, AMM has also been used for radial-field switched reluctance motor (SRM) [11]. In this study, a core loss reduction of about 63% was found at 8500 r/min, compared to the same machine using low loss silicon steel. The proposed SRM's efficiency was competitive with an interior PMSM (IPMSM). Induction motor (IM) core losses can also be diminished using AMM. In [12], AMM has been used to manufacture the stator core of an IM. A reduction of the core losses by almost 50% has been found at no-load and sinusoidal supplied voltage.

As for the PMSM type, it should be noted that, by now, AMM has been preferred for the axial-field type [9], [13]–[15] rather than radial-field PMSMs. In [13], the stator of the axial-field PMSM is made of several amorphous wound cores that are easy to manufacture and require few cutting. However, wound cores imply high core losses. Unfortunately, reducing these core losses requires more cutting [14], [15]. Moreover, highly performant axial-field PMSMs generally have a flat geometry (large diameter and little axial length) [16], which is not suited for all applications. In [17], AMM was used to build the stator teeth of a radial-field surface PMSM (SPMSM). The authors measured a core loss reduction of about 40% at 5500 r/min compared to the same PMSM made from conventional electrical steel sheets. A radial-field IPMSM using AMM has also been developed in [18]. Geometrical optimization allowed increasing the power density significantly compared to its equivalent made of silicon steel.

In this paper, a radial-field IPMSM with the entire stator core made of AMM is proposed. The rotor, however, is still made of conventional nonoriented (NO) electrical steel sheets.

TABLE I  
MATERIAL CHARACTERISTICS

	NO	AMM
Reference	35H300	2605HB1M
Composition	Fe-Si	Fe-Si-B
Thickness ( $\mu\text{m}$ )	350	25
Saturation magnetic flux density (T)	2.12	1.63
Resistivity ( $\mu\Omega\text{-m}$ )	0.5	1.20
Iron loss density at 50 Hz and 1 T (W/kg)	1.119	0.171
Iron loss density at 50 Hz and 1.5 T (W/kg)	2.419	0.400

Unlike [9] and [10], a low-speed application is presented here. It will be shown that AMM can be helpful in reducing core losses even at low speed. Compared to SRM [11] and IM [12], IPMSMs usually have higher efficiency and offer the advantage of a higher torque per volume. Therefore, it could be interesting to evaluate the potential benefit of AMM for an IPMSM also. As mentioned previously, the use of AMM is easier in axial-field PMSMs but this type of motor has a limited range of applications [16]. As a consequence, AMM is tried in a radial-field motor type here. Moreover, in [17], AMM has been used to build the stator teeth of an SPMSM. The work presented here differs from [17] in that the developed motor has interior permanent magnets (PMs) and has its full stator core made of AMM (not only the teeth). Finally, an IPMSM with a stator core made of AMM has been developed in [18] but the work did not focus on the core losses comparison with its equivalent made from conventional NO-silicon steel.

In this paper, the IPMSM core losses are defined by the summation of the stator, rotor, and magnets iron losses (hysteresis and eddy-current losses). It should be noted that in normal load condition, the copper losses can be much higher than the core losses in a PMSM. Then, even a rather big reduction of the core losses will lead to a small increase of the overall efficiency. However, a reduction of the core losses can be beneficial in some applications like electrical vehicles or hybrid electrical vehicles, where an electrical motor can be operated at zero torque or zero current. In these conditions, the core losses are the main contributor to the overall electrical motor losses. In addition, future electrical vehicles are likely to increase the rotational speed of their embedded electrical motor, making it work up to an electrical frequency of 1 kHz. Since the core losses increase with the operating frequency, they could become higher than the copper losses in some cases.

In this paper, the core losses are evaluated both experimentally and by finite-element method (FEM) under no-current condition. This test is useful to evaluate the core losses because no copper loss appears. The experimental data show a decrease of the core losses of about a half when compared to an IPMSM with a stator core made of NO-electrical steel sheets.

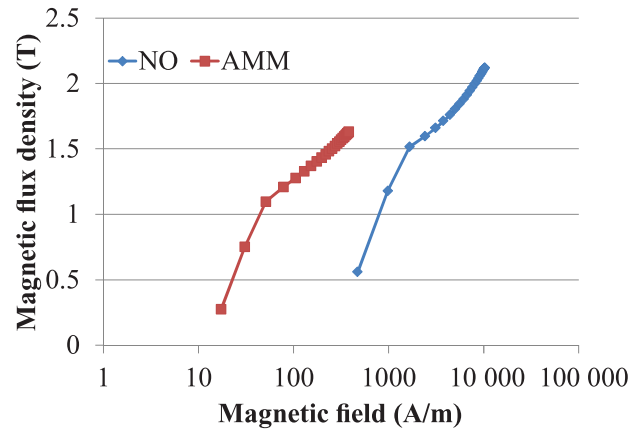


Fig. 1.  $B$ - $H$  curves of AMM and NO-materials.

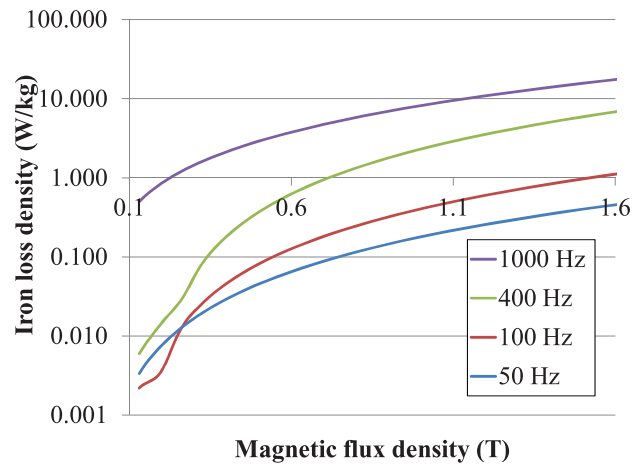


Fig. 2. Iron loss characteristic of the amorphous material.

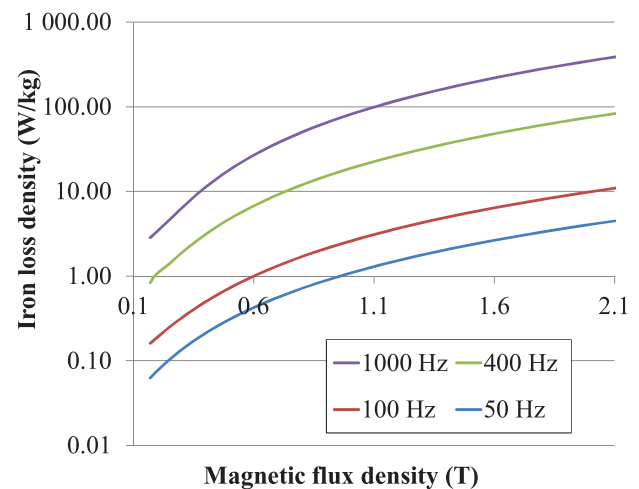


Fig. 3. Iron loss characteristic of the NO-material.

## II. MOTOR GEOMETRY AND MANUFACTURE

Two IPMSMs with identical geometries have been manufactured. The first, hereafter called NO-IPM, has a laminated stator made of standard NO-steel sheets, and the second, hereafter called AMM-IPM, has a laminated stator made of amorphous material. The material characteristics are described in Table I.

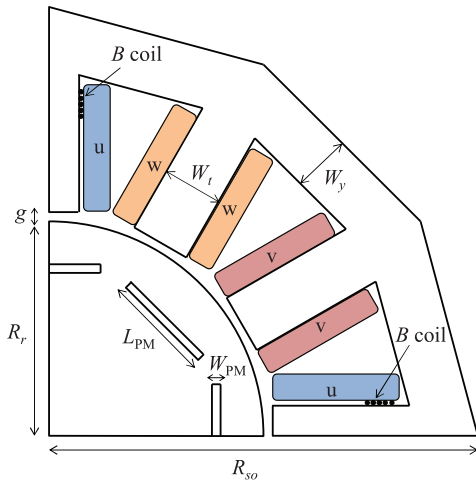


Fig. 4. Quarter cross-sectional view of the motor. The cross section of the full motor has horizontal and vertical reflection symmetries.

TABLE II  
MOTOR SPECIFICATIONS

Poles/slot number	8/12
Radius of stator core $R_{s0}$	64 mm
Radius of rotor core $R_r$	37 mm
Air gap $g$	1.25 mm
Yoke width $W_y$	9.2 mm
Tooth width $W_t$	10 mm
PM length $L_{PM}$	20 mm
PM thickness $W_{PM}$	2 mm
Core length $L_c$	47 mm
Winding method	Concentrated
Number of winding turns	37
PM residual magnetization	1.28 T
PM electrical resistivity	$1.6 \times 10^{-6} \Omega \cdot m$

Fig. 1 shows the  $B-H$  curves of both materials, where  $B$  is the magnetic flux density and  $H$  is the magnetic field. Figs. 2 and 3 show the iron loss density of both materials, which depends on the magnetic flux density and its frequency. These charts have been obtained by experimental measurements.

A cross-sectional view of the proposed motor is illustrated in Fig. 4 and the motor specifications are listed in Table II.

Since the amorphous ribbon is thin and brittle, special techniques have been adopted for the stator core manufacture. The manufacturing process is illustrated in Fig. 5. The amorphous sheets were first stacked and cut into the stator shape using a wire-cut technique. The cut stack was then placed into a vacuum box. After the vacuum was established, the cut stack was immersed into resin for lamination coating and bonding. The box was then submitted to high pressure to make the resin fill the interlaminations. Finally, the bonded stack was heated at a temperature of 180 °C for 150 min.

The two stators can be seen in Fig. 6. The stacking factor of the AMM stator core is 0.86 and that of the NO-stator is 0.99.

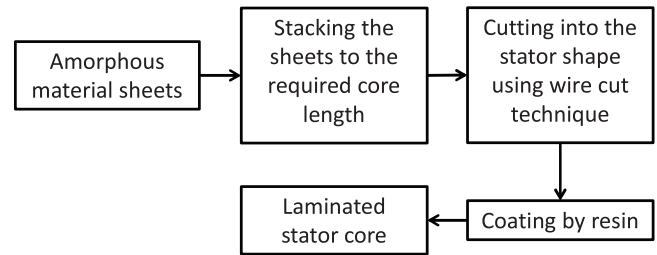


Fig. 5. Amorphous stator core manufacture process.

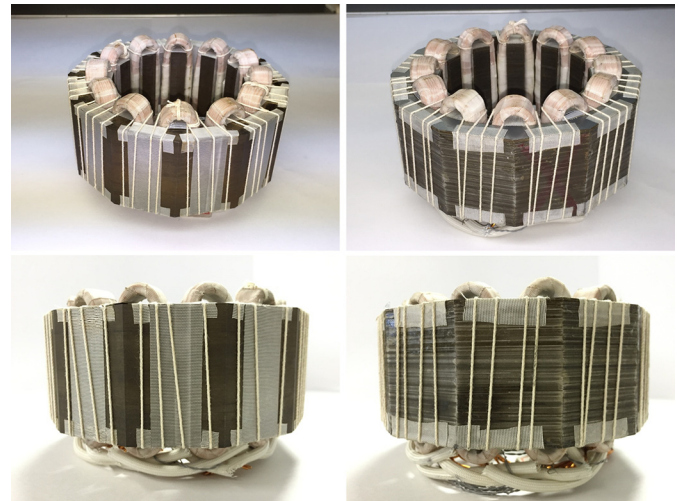


Fig. 6. (Left) AMM stator core and (right) NO-stator core.

### III. CORE LOSSES EVALUATION BY FEM

#### A. Numerical Analysis Method

The core losses of the two motors have been calculated by two-dimensional (2-D) magnetic field analysis using the JMAG simulation software. JMAG calculates the core loss density in the stator, rotor, and magnets at no-current condition by simulating the case in which the rotor of the IPMSM is rotated by an external motor and the three phases are in open circuit. Consequently, the core losses are caused by the rotating magnets. The simulation tool calculates the magnetic flux density and the core loss density  $W$  ( $W/m^3$ ) for several positions of the rotor spanning a total rotation angle of 90°, which corresponds to one electrical period.

In 2-D analysis, JMAG solves the vector potential equation based on the characteristic illustrated in Fig. 1. The equation is solved to find the magnetic flux density at each point of the motor cross-section. The 2-D vector potential equation is derived from Maxwell equation and is given by

$$\frac{\partial}{\partial x} \left( \nu_y \frac{\partial A_z}{\partial x} \right) + \frac{\partial}{\partial y} \left( \nu_x \frac{\partial A_z}{\partial y} \right) = -J_0 + \sigma \frac{\partial A_z}{\partial t} \quad (1)$$

where  $A_z$  is the vector potential on the  $z$ -axis,  $\nu_{x,y}$  are the magnetic reluctance on the  $x$ - and  $y$ -axis,  $J_0$  is the current density in the coil parts, which is equal to zero in this calculation, and  $\sigma$  is the electrical conductivity. In our case,  $\nu_x$  and  $\nu_y$  are equal since NO-material and AMM are considered magnetically isotropic.

To evaluate the core loss density  $W$ , JMAG first calculates the tangential component  $B_\theta$  and the radial component  $B_r$ ,

of the magnetic flux density at each point of the 2D motor cross section. A fast Fourier transform (FFT) is then performed to find the harmonic components of  $B_t$  and  $B_\theta$ . Finally, JMAG calculates the core loss density at each point using the Steinmetz equation

$$W = \sum_{i=1}^n (k_h f_i (B_{r,i}^2 + B_{\theta,i}^2) + k_e f_i^2 (B_{r,i}^2 + B_{\theta,i}^2)). \quad (2)$$

This equation is a sum through the harmonics of the magnetic flux density. At every point of the stator, rotor, and magnets, the magnetic flux density is usually not sinusoidal. In no-current condition, the stator slots shape and the rectangular magnets are responsible for harmonics [19]. Then, it is preferable to take these harmonics into account.  $i$  is the harmonic rank,  $n$  is the rank of the highest harmonic,  $f_i$  is the frequency of the  $i$ th harmonic,  $B_{r,i}$  and  $B_{\theta,i}$  are the amplitudes of the  $i$ th harmonic of the radial and tangential component of the magnetic flux density, respectively, and  $k_h$  and  $k_e$  are the Steinmetz constants of the hysteresis and eddy-current losses, respectively, which are derived from the data in Figs. 2 and 3.

It should be noted that the formulation in (2) calculates the alternating core losses only. However, the magnetic flux density is not only alternating but also rotating, making additional rotating core losses to appear [20]. Then for more accuracy, the calculation should consider the peak value of the radial component  $B_r$  and the tangential component  $B_\theta$  of the magnetic flux density, along with the magnetic flux variation locus. Ma *et al.* report that considering the rotational core losses in the numerical calculation can reduce the prediction error of 20% in average from 1000 to 4000 r/min, for an IPMSM with concentrated windings [21]. This percentage can also be considered as the proportion of the rotational core losses in the total core losses. It should be noted, however, that, contrary to the no-current condition of this paper, both calculations and experiments in [21] were performed under load condition with an armature current of 4 A. In [22], the core losses of a high-speed surface-mounted permanent-magnet motor with concentrated windings were modeled. By proposing a new model for the core losses numerical evaluation, it was found that the rotational core losses account for about 12.5% of the total core losses at 20 000 r/min. Both calculations and experiments in [22] were performed at no-load (small phase current).

It can be concluded from [21] and [22] that the rotational core losses have a non-negligible impact. However, an approximation similar to (2) has been used in [19] to evaluate the core losses of an IPMSM and the authors found a good agreement between experiment and calculation.

### B. Analysis Results

Figs. 7 and 8 show the peak flux density in one period and the maximum core loss density that occurs during the rotation, for a rotating speed of 750 and 3000 r/min, respectively. The magnetic flux density in the AMM stator core is slightly higher than the magnetic flux density in the NO-stator core but the values can be considered quite similar. However, the core loss density in the NO-stator core is significantly higher than the core

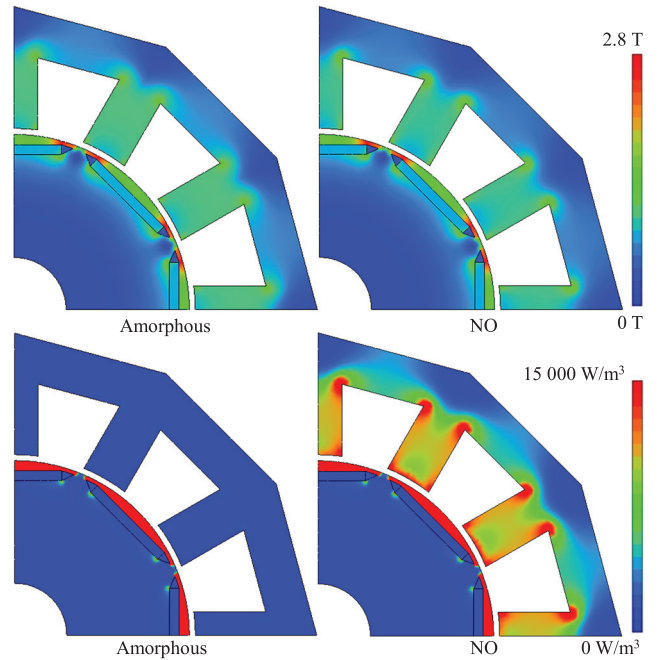


Fig. 7. (Top) Flux density and (bottom) core loss density at 750 r/min under no-current condition.

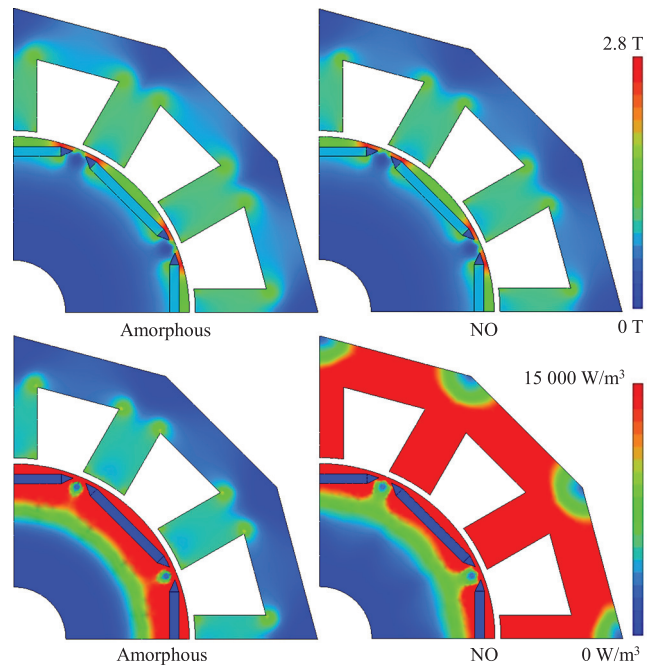


Fig. 8. (Top) Flux density and (bottom) core loss density at 3000 r/min under no-current condition.

loss density of the AMM stator core. Fig. 9 illustrates the magnetic field in the rotor and stator parts at 750 and 3000 r/min. The relative permeability of AMM and NO-silicon steel are quite different, which explains the difference observed on the magnetic field.

Table III shows the entire core losses of both motors calculated by the FEM software at the rotational speed values 750, 1500, 2250, and 3000 r/min. In average, the core losses of the AMM-IPM are 65% lower than the core losses of the NO-IPM.

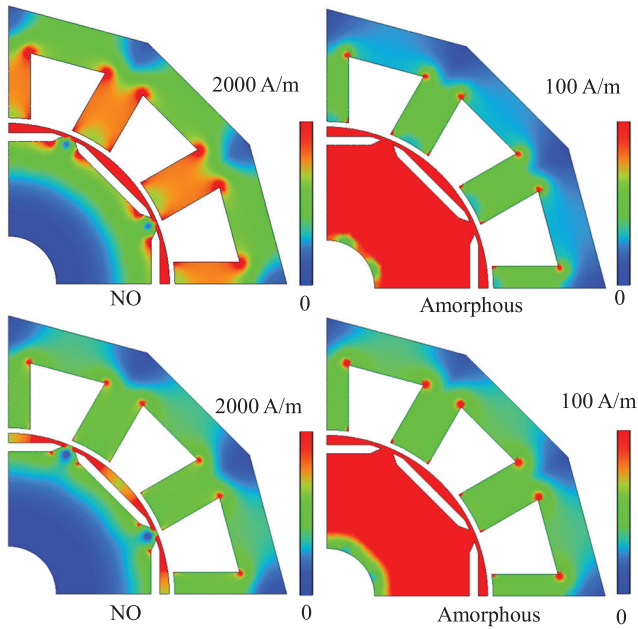


Fig. 9. Magnetic field at (up) 750 r/min and (bottom) 3000 r/min under no-current condition.

TABLE III  
CORE LOSS CALCULATION BY FEM

Speed (r/min)	AMM-IPM core losses (W)	NO-IPM core losses (W)
750	0.526	1.619
1500	1.420	4.133
2250	2.493	7.036
3000	3.783	10.473

Fig. 10 shows the core losses in the different parts of the motor at the same speed values, as in Table III. The average core loss reduction in the stator only is 83%. The ratio of core losses between the NO-IPM and the AMM-IPM is approximately 3 at every speed values. However, if one considers only the stator part, the ratio of core losses, which can be estimated using Fig. 10, clearly increases with the speed.

#### IV. CORE LOSSES EVALUATION BY EXPERIMENT

The experimental test bench for the no-current test is illustrated in Fig. 11. A brushless dc motor is used to rotate the AMM-IPM or the NO-IPM. A torque meter is placed between the two motors to measure the shaft torque  $T$  and a speed sensor measures the rotational speed  $\omega$ . The torque meter measures the material deformation and translates it into a torque value. The maximum torque that can be measured is 1 N·m and the maximum speed is 25 000 r/min. The three phases of the stator of the proposed IPMSM are in open circuit.

##### A. Magnetic Flux and Back EMF Measurement

As it can be seen in Fig. 4,  $B$  coils have been placed on the four teeth of the  $u$  phase coil. When the motor is rotating, the  $B$

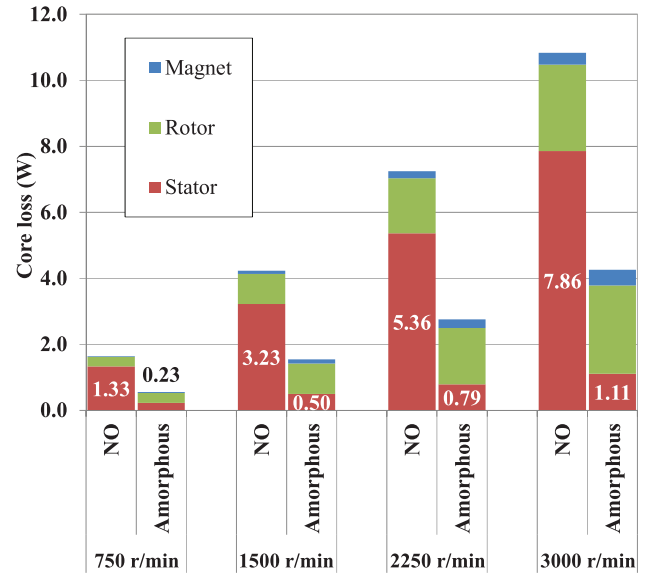


Fig. 10. Core losses in the different parts of the motor.

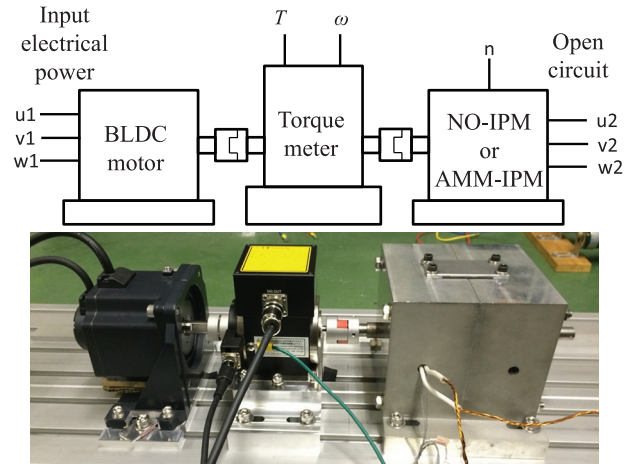


Fig. 11. Experimental test bench for the no-current test.

coils provide a periodic voltage  $V_B$  that can be used to calculate the average flux density through the tooth cross section  $B(t)$

$$B(t) = \frac{1}{N_B S_t} \int_0^t V_B(u) du \quad (3)$$

where  $N_B$  is the number of turns of the  $B$  coil and  $S_t$  is the tooth cross section surface given by

$$S_t = W_t L_c. \quad (4)$$

The magnetic flux density has been measured in both the NO-IPM and the AMM-IPM. The comparison is illustrated in Fig. 12 and shows the magnetic flux density along the electrical angle, which has been estimated using an additional encoder. The measurement has been done at 750 r/min but the peak flux density has been found almost independent from the rotational speed. In accordance with the FEM calculation, only a small difference can be observed between the two motors. This is due to the fact that the magnetic flux density is mainly imposed by the magnets and maintained below a level of 1 T. Even though

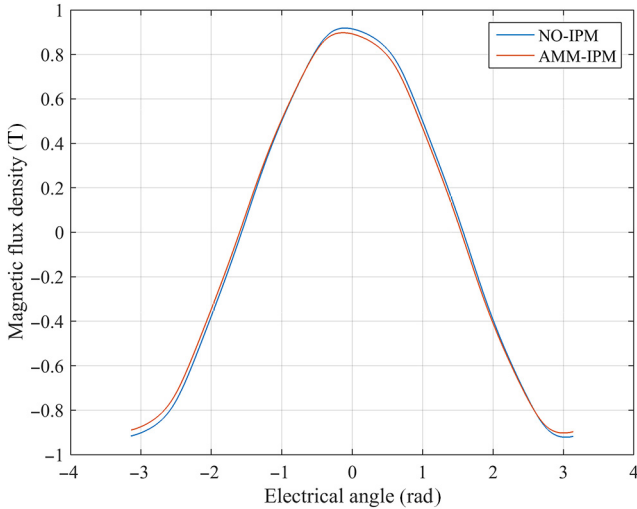


Fig. 12. Magnetic flux measurement in both motors.

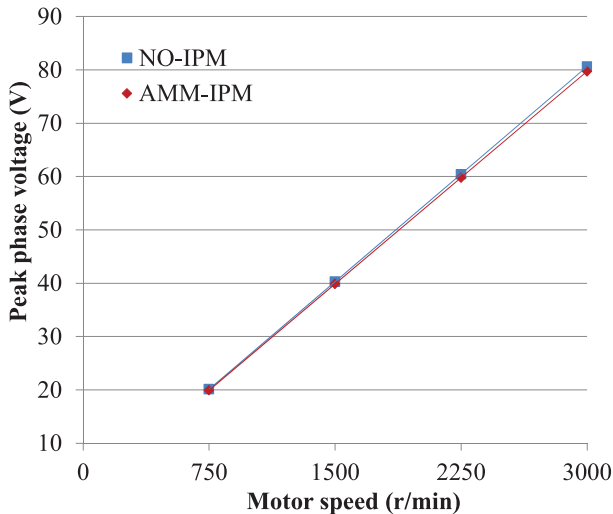


Fig. 13. Experimental back EMF measurement.

the magnetic saturation of AMM is lower than NO-steel, this saturation is not reached here and does not impact  $B$  in both motors.

The peak value of the back electromotive force (EMF) produced by the rotating magnets in the windings has also been measured at 750, 1500, 2250, and 3000 r/min. The results are illustrated in Fig. 13. It is possible to calculate the back EMF constant from the obtained curve. The constants of both motors are given in Table IV. They appear to be quite similar. This result is consistent with the measurement results of the magnetic flux. However, it cannot be concluded that the torque capacity is equivalent since saturation can appear at high input current. This paper focuses on the experimental tests with no-current, so the possible problem of magnetic saturation with current is not addressed here.

### B. Core Losses Measurement

Since no-current is flowing through the stator windings, the entire core losses are only produced by the magnet rotation. The

TABLE IV  
BACK EMF MEASUREMENT RESULTS

	AMM-IPM	NO-IPM
Back EMF constant (V/kr/min)	26.6	26.9

TABLE V  
CORE LOSS MEASUREMENT RESULTS

Speed (r/min)	AMM-IPM core losses (W)	NO-IPM core losses (W)
750	0.817	1.516
1500	1.963	3.864
2250	3.581	7.092
3000	6.000	12.472

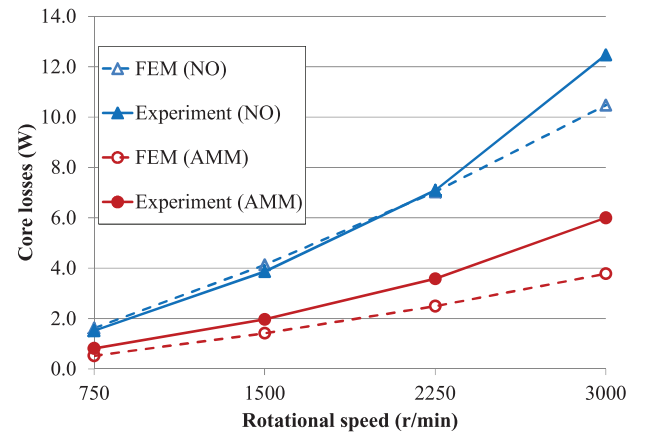


Fig. 14. Experimental core loss measurement.

output mechanical power of the brushless dc motor is equal to

$$\omega T = P_{\text{core}} + P_{\text{mech}} \quad (5)$$

where  $P_{\text{core}}$  is the core loss of the tested motor and  $P_{\text{mech}}$  is the mechanical friction loss.  $P_{\text{mech}}$  has first been measured using a rotor of the same shape without magnets (no-core losses), keeping identical bearings and couplings. Then, a second test has been carried out using the rotor with magnets. The core losses of both IPMSMs have been calculated by subtracting the value of  $P_{\text{mech}}$  measured during the first test from the output mechanical power measured during the second test.

The results are presented in Table V. In average, the core losses of the IPMSM with AMM stator core are approximately half the core losses of the IPMSM with NO-stator core. Moreover, a comparison between FEM calculation and experimental measurements is provided in Fig. 14. The measured core losses of the NO-IPM seem to be higher than the calculated ones at 3000 r/min. This could be due to the fact that the rotational core losses were not taken into account in the numerical calculation [21], [22]. As for the AMM-IPM, the measured core losses appear to be higher than the calculated ones for all speeds. Besides the consideration of the rotational core losses, it should be noted that part of this increase is also very probably due to the fact that the iron loss characteristic of AMM can

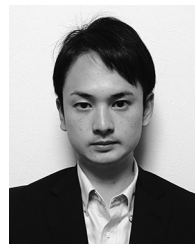
be deteriorated during the core manufacture process that causes mechanical stress. It should finally be added that both experimental data and FEM data are subject to uncertainties. To be conservative, it is better to rely on the experimental results and conclude that the amorphous stator core can reduce the motor core losses by about 50%.

## V. CONCLUSION

In this paper, an IPMSM using a stator made from amorphous material has been proposed. The core losses produced by magnet rotation have been measured experimentally and by numerical calculation. It has been found that a reduction of the core losses by about one-half can be obtained compared to the same motor using a conventional stator with NO-silicon steel sheets. Numerical calculation and experiments show a good agreement but it is thought that the mechanical stress during the AMM core manufacture is responsible for a deterioration of the material iron loss characteristics. Future work will concentrate on the core loss measurement when the motor is controlled by a three-phase inverter, both in no-load and load conditions. Some effort should also be put on improving the numerical calculation reliability.

## REFERENCES

- [1] H. Fujimori, H. Yoshimoto, T. Masumoto, and T. Mitera, "Anomalous eddy current loss and amorphous magnetic materials with low core loss," *J. Appl. Phys.*, vol. 52, no. 3, pp. 1893–1898, 1981.
- [2] A. J. Moses, "Demonstration of the feasibility of the use of amorphous magnetic material as transformer core material," in *Proc. 12th Int. Conf. Elect. Distrib.*, 1993, pp. 1–3.
- [3] V. Tsepelev, V. Konashkov, Y. Starodubtsev, V. Belozarov, and D. Gaipishevarov, "Optimum regime of heat treatment of soft magnetic amorphous materials," *IEEE Trans. Magn.*, vol. 48, no. 4, pp. 1327–1330, Apr. 2012.
- [4] Y. Okazaki, "Loss deterioration in amorphous cores for distribution transformers," *J. Magn. Magn. Mater.*, vol. 160, pp. 217–222, 1996.
- [5] R. Hasegawa, "Present status of amorphous soft magnetic alloys," *J. Magn. Magn. Mater.*, vols. 215–216, pp. 240–245, 2000.
- [6] S. R. Ning, J. Gao, and Y. G. Wang, "Review on applications of low loss amorphous metals in motors," *Adv. Mater. Res.*, vols. 129–131, pp. 1366–1371, 2010.
- [7] T. Suzuki, S. Itho, G. Terada, A. Chiba, M. Yoshida, and H. Watanabe, "Electric motor characteristic of SRM that uses heat-treated amorphous alloys accumulating body," *Proc. Inst. Elect. Eng. Jpn.*, RM-03-142, pp. 35–40, 2003.
- [8] S. H. Li, Z. C. Lu, D. R. Li, C. W. Lu, and S. X. Zhou, "Investigation on the core loss of amorphous stator core for high-speed motor," *Small Spec. Elect. Mach.*, no. 6, pp. 24, 2009.
- [9] Z. Wang, Y. Enomoto, R. Masaki, K. Souma, H. Itabashi, and S. Tanigawa, "Development of a high speed motor using amorphous metal cores," in *Proc. IEEE 8th Int. Conf. Power Electron.—ECCE Asia (ICPE/ECCE'11)*, Jeju, 2011, pp. 1940–1945.
- [10] R. Kolano, K. Krykowsky, A. Kolano-Burian, M. Polak, J. Szynowski, and P. Zackiewicz, "Amorphous soft magnetic materials for the stator of a novel high-speed PMBLDC motor," *IEEE Trans. Magn.*, vol. 49, no. 4, pp. 1367–1371, Apr. 2013.
- [11] A. Chiba *et al.*, "Test results of an SRM made from a layered block of heat-treated amorphous alloys," *IEEE Trans. Ind. Appl.*, vol. 44, no. 3, pp. 699–706, May/June. 2008.
- [12] M. Dems and K. Komez, "Performance characteristics of a high-speed energy-saving induction motor with an amorphous stator core," *IEEE Trans. Ind. Electron.*, vol. 61, no. 6, pp. 3046–3055, Jun. 2014.
- [13] Z. Wang *et al.*, "Development of a permanent magnet motor utilizing amorphous wound cores," *IEEE Trans. Magn.*, vol. 46, no. 2, pp. 570–573, Feb. 2010.
- [14] G. S. Liew, W. L. Soong, N. Ertugrul, and J. Gayler, "Analysis and performance investigation of an axial-field PM motor utilising cut amorphous magnetic material," in *Proc. 20th Australas. Univ. Power Eng. Conf.*, Christchurch, New Zealand, 2010, pp. 1–6.
- [15] Z. Wang *et al.*, "Development of an axial gap motor with amorphous metal cores," *IEEE Trans. Ind. Appl.*, vol. 47, no. 3, pp. 1293–1299, May/June. 2011.
- [16] A. Cavagnino, M. Lazzari, F. Profumo, and A. Tenconi, "A comparison between the axial flux and the radial flux structures for PM synchronous motors," *IEEE Trans. Ind. Appl.*, vol. 38, no. 6, pp. 1517–1524, Nov./Dec. 2002.
- [17] Y. Enomoto *et al.*, "Evaluation of experimental permanent-magnet brushless motor utilizing new magnetic material for stator core teeth," *IEEE Trans. Magn.*, vol. 41, no. 11, pp. 4304–4308, Nov. 2005.
- [18] T. Fan, Q. Li, and X. Wen, "Development of a high power density motor made of amorphous alloy cores," *IEEE Trans. Ind. Electron.*, vol. 61, no. 9, pp. 4510–4518, Sep. 2014.
- [19] K. Yamazaki and Y. Seto, "Iron loss analysis of interior permanent-magnet synchronous motors—variation of main loss factors due to driving condition," *IEEE Trans. Ind. Appl.*, vol. 42, no. 4, pp. 1045–1052, Jul./Aug. 2006.
- [20] M. Enokizono, T. Suzuki, J. Sievert, and J. Xu, "Rotational power loss of silicon steel sheet," *IEEE Trans. Magn.*, vol. 26, no. 5, pp. 2562–2564, Sep. 1990.
- [21] L. Ma, M. Sanada, S. Morimoto, and Y. Takeda, "Prediction of iron loss in rotating machines with rotational loss included," *IEEE Trans. Magn.*, vol. 39, no. 4, pp. 2036–2041, Jul. 2003.
- [22] Y. Huang, J. Dong, J. Zhu, and Y. Guo, "Core losses modeling for permanent-magnet motor based on flux variation locus and finite-element method," *IEEE Trans. Magn.*, vol. 48, no. 2, pp. 1023–1026, Feb. 2012.



**Shotaro Okamoto** was born in Fukuoka, Japan, in 1987. He received the B.Eng. degree in engineering from the Toyota Technological Institute, Nagoya, Japan, in 2015.

Since 2008, he has been with Toyota Motor Corporation, Toyota City, Japan, as a Development Engineer for hybrid vehicles. His research interests include development of a high-efficiency amorphous motor and the evaluation of its losses.



**Nicolas Denis** (M'12) was born in 1987. He received the M.Eng. degree and the French Engineer Diploma degree in electrical engineering from the École Nationale Supérieure d'Électricité et de Mécanique de Nancy, Nancy, France, in 2010, and the Dr. Eng. degree in electrical engineering from Sherbrooke University, Sherbrooke, QC, Canada, in 2014.

He is currently a Postdoctoral Fellow with the Toyota Technological Institute, Nagoya, Japan, and works on the application of efficient magnetic materials for electrical motors.



**Yoshiyuki Kato** was born in Tokyo, Japan, in 1992. He has been working toward the B.Eng. degree in engineering at the Toyota Technological Institute, Nagoya, Japan, since 2011.

His research interests include the evaluation of the iron losses of interior permanent-magnet synchronous motors under inverter excitation by measurement and numerical magnetic analysis.



**Masaharu Ieki** was born in 1992. He has been working toward the B.Eng. degree in engineering at the Toyota Technological Institute, Nagoya, Japan, since 2011.

His research interests include the evaluation of the drag loss of interior permanent-magnet synchronous motors at high speed (up to 10 000 r/min); magnetic cores using conventional silicon steel magnetic material and amorphous magnetic material are both investigated.



**Keisuke Fujisaki** (S'82–M'83–SM'02) was born in 1958. He received the B.Eng., M.Eng., and Dr.Eng. degrees in electronics engineering from The University of Tokyo, Tokyo, Japan, in 1983, 1986, and 1987, respectively.

In 1986, he was with Nippon Steel Corporation. Since 2010, he has been a Professor with the Toyota Technological Institute, Nagoya, Japan. From 2002 to 2003, he was a Visiting Professor at Oita University, Oita, Japan. From 2003 to 2009, he was a Visiting Professor at Tohoku University, Sendai, Japan. His

research interests include magnetic multiscale and electromagnetic multiphysics, including electrical motors, electromagnetic material processing, and electrical steel.

Dr. Fujisaki was the recipient of the Outstanding Prize Paper Award at the Metals Industry Committee sessions of the 2002 IEEE Industry Applications Society Annual Meeting.